Molecular dynamics simulation of synchronization in driven particles

Tiare Guerrero* and Danielle McDermott†
Department of Physics, Pacific University, Forest Grove, OR 97116
(Dated: January 16, 2021)

Synchronization plays a key role in many physical processes. Modeling synchronization with simulations and table-top experiments can provide insight to complex behaviors in the natural world. Driving particles across a washboard potential energy landscape is a common technique to isolate complex synchronized patterns in both simulations and experiments. We discuss a simple numerical model using molecular dynamics simulations for particles moving through a viscous liquid. Our results show a variety of synchronization effects in single and multi-particle systems, which we characterize with plots of particle velocity as a function of applied driving force, and phase diagrams of position versus velocity.

I. INTRODUCTION

Synchronization is a universal phenomena in which individual oscillators adjust frequency due to external stimulus [1]. Many everyday systems exhibit in-phase coupled oscillations such as the flickering patterns of candle flames mediated by temperature fluctuations [3], vibrations of singing wineglasses interacting through sound waves [4], and metronomes vibrating through a supporting platform [5]. Biological systems benefit from cooperative synchronization – birds coordinate wing flaps to optimize energy use during flight [6], frogs alternate croaking patterns [7], humans clap in time with music [8] and at a cellular level, neurons simultaneously fire in cardiac muscle [9] and brain tissue [10]. External forcing can cause or regulate synchronization. For instance, an electrical pacemaker pulses to regulate a heart beat, and a flashing light can modify the pattern of flashing fireflies .

A particular form of synchronization is phase-locking or mode-locking, which first appeared in the scientific literature with Huygens' 1665 experiments on the motions of two wall-mounted pendulum clocks. Huygens demonstrated the tendency of the pendula to swing in time, even when started out of phase, due to interactions through the wall [2]. Dynamical systems exhibit phase-locking when oscillators with different rhythms adjust to a frequency ratio or mode of an integer number [12]. Synchronization is often studied with simple computational models and can be visualized with phase plots or Lissajous figures. In phase space a mode-locked system is confined to a closed loop in a parametric space showing the relationship between two periodic functions with patterns determined by the mode, first reported in 1857 [13] and easily generated with a computer code or oscilloscope [14]. It should be noted that the term phase has two scientific meanings, "oscillation phase" and "phase space" Oscillation phase ϕ_0 is the constant portion of the argument in a periodic function $\sin(\omega t + \phi_0)$ while phase space refers to plots of velocity versus position (such as v_y vs. y) that are used to characterize oscillating systems.

Here we perform numerical studies on the synchronized dynamics of confined particles driven over a washboard shaped potential energy landscape. We chose this model for its relevance to condensed matter systems and ease of simulation. In Section II we describe colloid particles, an relevent experimental analog of our simulations. We describe our molecular dynamics model for a single particle in Section III. We summarize our results including synchronized motion of a single confined particle driven across a periodic landscape in Section IV. In Section VIII we extend the model to include multiple particles, and show how confined interacting particles respond to the same applied driving force. In Section VI we describe how our work with colloids applies more broadly to many physical systems such as dusty plasmas, superconducting vortices and Josephson junctions. We conclude with exercises for interested students in Section V.

II. COLLOIDAL MODELS

Complex dynamics can be studied with colloid particles with experiments and simulation. In typical experiments colloids are spheres of plastic suspended in highly de-ionized water or silica in suspended in organic solvent. Because the spheres are a few microns in size and move at rates of microns per second, the position of a particle can be imaged as a function of time with a traditional optical camera. Individual colloids exhibit Brownian motion, where particles change direction due to collisions with unseen particles comprising the suspending fluid [].

Light is a tool for manipulating the colloidal environment. A single laser beam can be used to create an optical trap, which uses photon radiation pressure to control colloid motions [30]. A circular optical trap is designed with a local energy minimum at its center. A colloid in the beam center is subject to a uniform distribution of photon bombardment, and motions away from the center create a net force due to an uneven distribution of photon collisions on its surface. Depending on the location of the particle in the trap, the radiation pressure either restores colloids toward the local minima or ejects it from the trap. A single optically trapped colloid exe-

*Electronic address: guer9330@pacificu.edu
†Electronic address: mcdermott@pacific.edu

cuting Brownian motion is a useful probe of microscopic forces, and has been studied in detail in Ref. [31].

In experiments complex environments can be engineered with light by using diffraction gratings to create a patterned potential energy landscape with one or more laser beams []. Experiments of colloid particles confined in optical traps arrays or patterns subject to external driving forces have been used to examine the microscopic dynamics of individual particles during mode-locking [25]. This produced step-by-step diagrams of particle dynamics that cannot be imaged in electronic systems such as Josephson junctions. Thus the study of mode-locking is a useful problem of complex quantum mechanical systems.

Numerical modeling of colloids can provide mechanistic insight that can be difficult to achieve in experimental conditions where Brownian motion and other sources of noise dominate.

III. MOLECULAR DYNAMICS SIMULATION

We use a classical model for studying the dynamics of N interacting particles, using the net force on each particle to calculate its trajectory. Particles are confined in a two-dimensional (2D) simulation of area $A = L \times L$ where $L = 36.5a_0$ where a_0 is a dimensionless unit of length. An individual particle i has position $\vec{r}_i = x_i\hat{x} + y_i\hat{y}$ and velocity $\vec{v}_i = d\vec{r}_i/dt$. The edges of the system are treated with periodic boundary conditions such that a particle leaving the edge of the system is mapped back to a position within the simulation boundaries by the transformation $x_i + L \to x_i$ and $y_i + L \to y_i$. We show a schematic of the system in Fig. 1(a).

We confine the particles using a position dependent potential energy function, called a landscape or substrate. The landscape is modulated in the y-direction with the periodic function

$$U(y) = U_0 \cos\left(N_p \pi y/L\right) \tag{1}$$

where N_p are the number of periods, and U_0 is an adjustable parameter to set the depth of the minima with simulation units of energy $E_0 = 1$. We plot this function in Fig. 1 for $N_p = 3$. In Fig. 1(a) we show the $x-y$ plane with a contour plot of $U(y)$ to illustrate the 2D potential energy landscape, where the maxima are colored red and the minima colored blue. The confining force on a particle i is calculated as $\vec{F}_i^l(\vec{r}_i) = -\nabla U_l(\vec{r}_i)$. In Fig. 1(b) we plot the function $U(y)$ to illustrate how the magnitude $\vec{F}_i^l$ is calculated from particle position y_i.

Particles are subject an external time-dependent driving force $\vec{F}_D(t)$ applied parallel to the y-direction. We model this force as

$$\vec{F}^d(t) = [F^{dc} + F^{ac}\sin(\omega t)]\hat{y}, \tag{2}$$

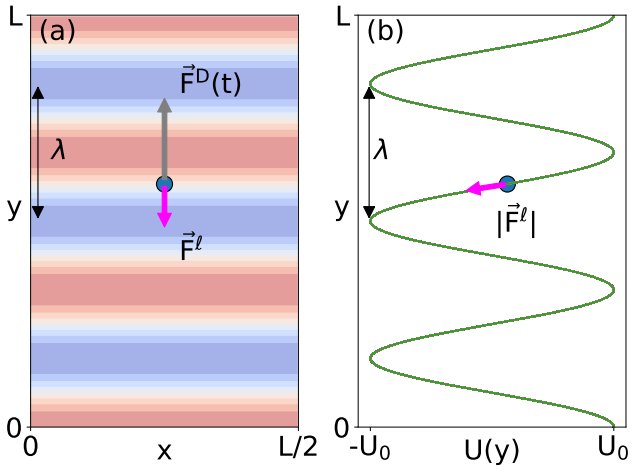

FIG. 1: Schematic of the simulation of a single particle driven across a washboard potential energy landscape. The period of the landscape is $\lambda = L/N_p$, where $N_p = 3$. The force due to the landscape is calculated from the gradient of the potential energy $\vec{F}^l = -\nabla U(\vec{r})$. (a) View of the $x-y$ plane. The time-dependent applied driving force $\vec{F}^d$ is parallel to the y-axis. The landscape is shown with a contour plot, with maxima in the potential energy marked in red and minima marked in blue. A particle is shown in the region between minima and maxima subject to competing forces of the landscape and applied driving force. (b) The potential energy function along the y-axis $U_l(y)$. The particle in (a) is shown at the same $y-$position. The slope of $U_l(y)$ is the magnitude of force $\vec{F}^l$.

with modifiable parameters including a constant component F^{dc}, and a time dependent component with amplitude F^{ac} and frequency $\omega = 2\pi f$.

The inertia of small particles is reduced by interactions with fluid particles [15]. In this model colloids are overdamped – i.e. suspended in a continuous viscous fluid that dissipates energy such that the particles do not accelerate. Energy dissipation from the fluid is modeled with a frictional force on particle with velocity $\vec{v}_i$ $\vec{F}_i^{drag} = -\eta\vec{v}_i$ with a friction coefficient η proportional to the fluid viscosity. We discuss friction models for spheres moving through fluids in Exercise 1. Newton's second law for an individual particle is simplified by the assumption $\vec{a}_i$ is zero. The overdamped equation of motion for an isolated particle is

$$\eta\vec{v}_i = \vec{F}_i^l(\vec{r}_i) + \vec{F}^d(t). \tag{3}$$

with $\eta = 1$. The equation of motion provides a direct calculation of the velocity of an individual particle from its location $\vec{r}_i$ and the simulation time.

The molecular dynamics simulation is controlled by a $for()$ loop which runs from an initial to maximum integer number of time steps. Each integer time step interval represents a simulation time interval of Δt simulation units. At each time step we evaluate the net force on each particle as a function of its position $\vec{r}_i(t)$ and then integrate the equation of motion to move particles to an

updated position. Since the acceleration as zero, the integration of the equation of motion is performed via the Euler method

$$\vec{r}_i(t+\Delta t) = \vec{v}_i(t)\Delta t + \vec{r}_i(t) \tag{4}$$

for a small time step $\Delta t = 0.001\tau$. In Exercise 2 we describe the numerical methods for solving differential equations. The units of the simulated variables are summarized in Table I.

TABLE I: Simulation units and approximate values in experiment. (coming soon!)

Quantity	Simulation Unit	Experimental range
length	$a_0 = 1$	$< a_0 <$
energy	$E_0 = 1$	$< E_0 <$
force	$F_0 = E_0/a_0$	$< F_0 <$
velocity	a_0/τ	$< v <$
viscosity coefficient	$\eta = F_0\tau/a_0$	$< \eta <$
time	$\tau = \eta a_0/F_0$	$< \tau <$

IV. MODE-LOCKING OF A SINGLE PARTICLE

A single particle responds to the applied driving force by moving across the landscape synchronized with the period of $F^d(t)$. The numerical implementation of the landscape is calculated with Eq. 1 as

$$F^l_y(y) = -A_p \sin\left(N_p \pi y/L\right) \tag{5}$$

where the force is scaled with parameter A_p. When $F^d(t) > A_p$, a particle can overcome the barrier height of the landscape, and the particle hops between minima in the energy landscape. In this section, we fix the landscape parameters to $A_p = 0.1$ force units with $N_p = 20$ minima in the landscape corresponding to a spatial period $\lambda = 1.825a_0$.

In Fig. 2 the driven particle adjusts its motion to traverse the periodic landscape with the same rhythm as the applied time-dependent force $F^d(t)$. In Fig. 2(a) we plot $F^d(t)$ as a function of time with constants $F^{dc} = 0.1$, $F^{ac} = 0.05$ and $f = 0.01$ cycles per time unit τ. The temporal period of the driving force is $T = 1/f = 100\tau$. We mark the maxima of $F^{ac}(t)$ with the vertical dashed lines – i.e. $\sin(\omega t) = 1$.

In Fig. 2(b) we show the $y-$position of the particle as a function of time. We normalize y by λ, the spatial period of the potential to show how the particle moves between substrate minima. The initial particle position is $y = 1a_0$, where the F^l is negative. As the driving force increases, the motion of the particle synchronizes with the driving period T. The particle moves in the positive y-direction through $\Delta y = 2\lambda$ over the time period T, with the average velocity $\langle v_y \rangle = 2\lambda f$. The horizontal dashed lines coincide with the condition the substrate force is minimum $F^l = -A_p$, i.e. $\sin(\pi y/\lambda) = 1$. The driving force is maximum when the landscape force on the particle is minimum, as indicated with the coincidence of the particle position y with the intersection of the horizontal and vertical lines. The slope of y/λ is proportional to the net force on the particle. This can be seen in Fig. 2 where local extrema appear in y/λ when $F_D(t) \approx 0$.

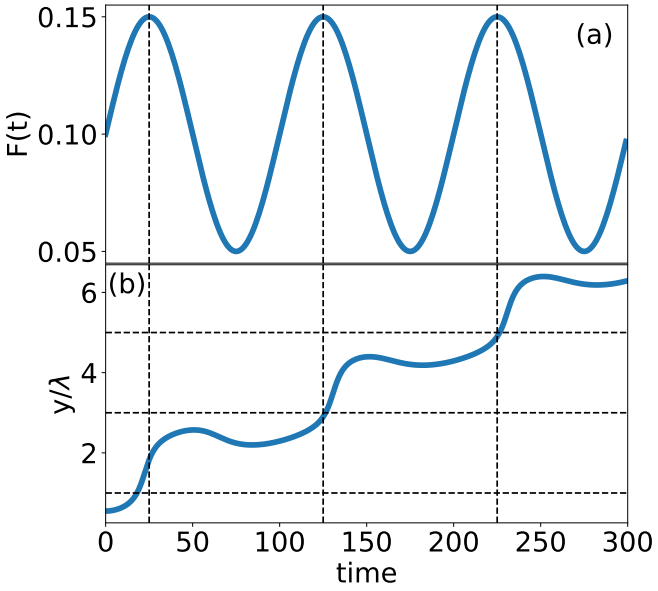

FIG. 2: (a) The applied driving force $F^d(t)$. (b) The $y-$position of the driven particle as a function of time normalized by the period of the substrate λ.

The competition between the driving force and landscape potential can produce a variety of hopping patterns in the particle motion. The relative values of F^{ac}, F^{dc} and A_p control the rate and distance a particle moves forward and backward in the landscape. To explore the possible hopping patterns, we sweep through a range of F^{dc} for fixed F^{ac} and A_p, as shown in Fig. 3(b). We keep F^{dc} constant for 10^5 simulation timesteps and measure the average velocity $\langle v_y \rangle$ as a function of F^{dc}. The average velocity $\langle v_y \rangle$ is the average displacement over the period of the driving force. We plot the results in Fig. 3 for $F^{ac} = 0.05$, $f = 0.01$, and the landscape shown in Fig. 2. Discrete steps in $\langle v_y \rangle$ occur because the average velocity of the particle is constant across a range of F^{dc}. This synchronization of the particle velocity can be measured in terms of the landscape period. Each step represents a different pattern of hops between substrate minima performed by the particle.

If A_p is large compared to the extrema of $F^d(t)$, the particle oscillates back and forth in a single minima with no net velocity. In Fig. 3, this occurs at low F^{dc} when $\langle v_y \rangle$ is zero.

The particle achieves a variety of oscillation modes as a function of F^{dc}. A mode is a periodic pattern of hops with a constant average particle velocity, $\langle v_y \rangle$ over a range of driving forces F^{dc}. We illustrate mode-locking in the velocity-force plot in Fig. 3. Here $\langle v_y \rangle$ is increasing in non-uniform steps, with a quantized height of $\langle v_y \rangle = n\lambda f$, where n is an integer.

Phase locked steps occur for average displacements integer multiples of the substrate period $n\lambda$.

We explore a range of parameters in Ex. 5 where we perform this sweep for several values of F^{ac} including the limiting case that the applied force is a constant value. When $F^{ac} = 0$, no steps appear in the $\langle v_y \rangle$ vs F^{dc} curve. When $F^{dc} - F^{ac} < -A_p$ the particle moves in the negative y-direction during part of the cycle.

We show the dynamics in supplementary materials [38].

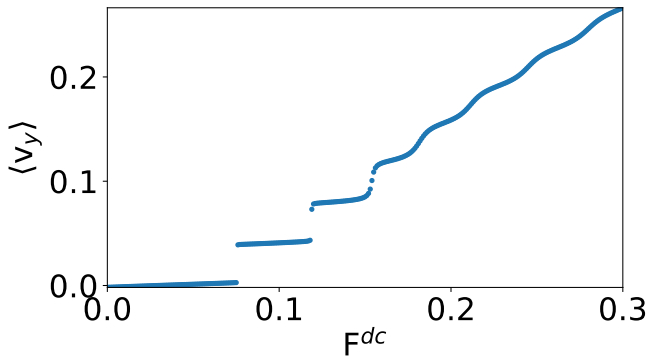

FIG. 3: Average particle velocity $\langle v_y \rangle$ as a function of F^{dc}, the constant parameter of $F^d(t)$ defined in Eq. 2. The remaining parameters in $F^d(t)$ are as in Fig. 2, $F^{ac} = 0.05$ and $f = 0.01$.

The period of the substrate can be used to control the intrinsic velocity of the dc driven particle, and the applied ac drive can cause mode-locking which appears as non-linear steps in the force-velocity relationship.

Fundamental models of synchronization can include many coupled oscillators or focus on a single particle driven across a periodic potential landscape. Single particle studies are useful to understand synchronization in the absence of collective effects. The relationship between the driving force and landscape can change the pattern of motion. With a constant or dc drive the landscape modulates the particle velocity, below some threshold the dc force is not strong enough to push the particle across a potential maximum so the average velocity is zero, a phenomena refered to as pinning [23]. A sinusoidal or ac drive creates mode-locking, where the average particle velocity is fixed for a range of dc drive forces [24].

V. ASSOCIATED PROBLEMS

1. Stokes' law describes the viscous drag on a sphere moving at velocity $\vec{v}$ as $\vec{F}^{lin} = 3\pi\eta D\vec{v}$ [] where η is the dynamic fluid viscosity and D is the particle diameter. (In simulation we subsume the constants $3\pi D$ such that $\eta \to 3\pi D\eta$.) Often drag forces are modeled as a polynomial series $\vec{F}^{drag} = \vec{F}^{lin} + \vec{F}^{quad} + ...$ Truncating the series to the first term is justified by calculating the Reynolds number $R = Dv\rho/\eta$ where ρ is the fluid density and v the particle's speed. When R is small, the quadratic and higher order drag terms may be ignored in favor of the linear drag term.

   Demonstrate the Reynolds number is low for this system.

   Reasonable experimental values for a colloid are $D = 1\mu m$ and $v \sim 1\mu m/s$. Viscosity of water decreases with temperature from $1.3 \times 10^{-3} Pa - s$ at $10°C$ to from $0.31 \times 10^{-3} Pa - s$ at $90°C$, making $\eta \sim 10^{-3} Pa - s$, where 1 pascal $= 1Pa = 1N/m^2$. Likewise the density ρ varies with temperature and $\rho \sim 10^3 kg/cm^3$ is a reasonable approximation.

   [citation for these values better than wikipedia] []

   This model should be familiar to readers of a standard classical mechanics text, such as Ref. [37] when studying models Millikan's oil drops.

   [could certainly do more with this question to make it more computational. For instance, plot R as a function of any of the parameters v, D and ρ, include a temperature dependent $\eta(T)$ in the Brownian system. Suggest students model something big and include inertia and quadratic drag, but then we're fairly off topic...]

2. Equation of Motion and Integration Methods

   Newton's second law states that the acceleration of a particle i is proportional to the sum of forces on a particle

$$m_i\vec{a}_i = \sum \vec{F}_i \tag{6}$$

   where the constant of proportionality is the inertial mass m_i The addition of a dissipative force in a dynamical model on a colloid is typically modeled with a drag force proportional to the particle's velocity in the opposite direction of motion $\vec{F}^{drag} = -\eta\vec{v}_i$ where η is the drag coefficient. Demonstrate the ratio of m/η has units of time, known as the momentum relaxation time. The momentum relaxation time is known to be small for particles with low Reynolds numbers, indivating a regime in which the acceleration term can be ignored entirely. Demonstrate that a particle confined to a landscape exerting force $F^l(\vec{r}_i)$ subject

to a time dependent drive $F^d(t)$ can be modeled with the equation of motion described in Eq. 11.

Generally when solving differential equations, the Euler method is effective for solving linear equations, such as the one-dimensional $f(y) = df/dy$ but not higher order methods.

The Verlet method simplifies to

and demonstrate how the Verlet method simplifies to the Euler method when $\vec{a} = 0$.

Because we are performing molecular dynamics for a single particle on a smooth potential energy landscape, we use a large simulation time step of $\Delta t = 0.01$. In Sec. VIII, we decrease the time step to treat multiple particle interactions.

We invite interested students to repeat this simulation for any initial particle position and a range of simulation constants to demonstrate that synchronization in this model does not depend on a particular set of conditions.

3. Drawing the contour

   The code for generating a two dimensional colored plot of the potential landscape is calculated by evaluating the analytic function in Eq. **??** for a grid of values (x_n, y_n).

4. **Brownian motion** is a temperature and viscosity dependent phenomena. [] Consider the consequences of a non-zero temperature on the simulation, in which particles will collide with invisible particles making up the suspending fluid. These collisions are more likely at higher temperature due to the increased kinetic energy of the fluid particles, as described by the Maxwell-Boltzmann distribution []. In molecular dynamics simulations temperature effects can be modeled by including randomized forces f^T to emulate the motion of particles undergoing Brownian motion. A distribution of randomizes forces contributes equally in all directions such that the force averaged over a finite time interval is zero $\langle f^T(t)\rangle = 0$. Random distributions of contain no correlations over the independent variable (time in this case) $\langle f^T(t) f^T(\tau)\rangle = 2\eta k_B T \delta(t-\tau)$ where the energy $k_B T$ derived from the Boltzmann constant k_B and temperature T has energy units E_0. [36]

   With no applied driving force, measure the minimum temperature required for a single particle to hop between minima in the potential landscape.

   Measure the rate of diffusion.

5.

6. Frenkel-Kontorova and competing length scales for low temperature systems where thermal fluctuations are negligible

7. The Fokker-Planck Equation

8. Aubrey-Kontorova + commensurability

9. nanotribology

   kink motion Vanossi et al J.Phys.: Condens. Matter 19 (2007)

VI. CONCLUSION

Our simulations reproduce results presented in Juniper *et al.* [25, 26] which demonstrated mode locking in experiments and simulations of driven colloids on a optical periodic landscape. Due to the relative ease of manipulation and imagining, colloids are used as experimental models for systems relatively hard to access and visualize. Collections of colloids can be used to study the properties of solids and liquids or more exotic systems such as cold atoms or electron gases [29].

Dynamical mode-locking is observed in quantum electronic devices such as Josephson junctions [16, 17]. A single junction contains two superconductoring layers which sandwich an insulating layer. When subject to an external voltage, Cooper pairs in the superconducting materials tunnel through the insulating layer. Phase-locking is observed as stepped regions in current-voltage (I-V) relationship in these devices, where voltage is the analog of external driving force and current is that of particle velocity. Known as Shapiro steps, these phase locked currents have been observed due to applied ac voltages in single Josephson junctions [19, 21] and coupled arrays of junctions [20]. Shapiro steps vary in width depending on the strength of the applied ac forces, and are observed in a variety of systems displaying non-Ohmic behavior in voltage-current curves, including ac and dc driven charge and spin density waves.

VII. SUPPLEMENTARY MATERIALS

VIII. SYNCHRONIZED PARTICLE CHAINS

The interaction forces between colloids can be controlled by altering the chemistry of the suspending fluid or surface ligands of the particles. Thus colloids can be modified to mimic different systems such as hard spheres interacting via contact forces [], dipole interactions [], and long range electrostatic interactions [].

Mode-locked colloid dynamics have been achieved in experiments [25, 32] and simulations [27, 28] for a variety of interaction types such as magnetic dipoles and electric forces.

Particles in confined geometries behave differently than free particles. Stabilized charged particles form patterns due to the interplay of the confining landscape and particle interactions. Narrow channels studies are useful to provide insights of how particles move through systems

such as charge carries in quantum wires [33] and slime molds in microchannels [34]. In multi-particle simulations, we confine the particles to a narrow region along the $x-$direction using a periodic function

$$U_{q1D}(x) = U_{q0}\cos(\pi x/L) \tag{7}$$

where U_{q0} defines the channel depth. This quasi-one-dimensional geometry confines the particles primarily to move along the y-direction but allows for some lateral motion of particles. Otherwise the repulsive interaction between particles would cause them to spread throughout the system. The total landscape potential energy function is the sum

$$U_{landscape}(x,y) = U_{q1D}(x) + U_{washboard}(y) \tag{8}$$

We explore collective effects in a twenty particle system confined to a narrow channel, as shown in Fig. 2a). We create the confining channel with a sinusoidal function with a single period.

$$U_l(x) = U_{0x}\cos(\pi x/L). \tag{9}$$

The landscape potential energy is illustrated in Fig. 4(a) where red regions are high potential and blue regions are low potential.

We model particle interaction forces $\vec{F}_{ij} = -\nabla U_{ij}(r_{ij})$ with the Yukawa potential $V_{ij} = U_{ij}/q$

$$V_{ij}(r_{ij}) = \frac{E_0}{r_{ij}} e^{-\kappa r_{ij}}, \tag{10}$$

where particle i and j are distance $r_{ij} = |\vec{r}_i - \vec{r}_j|$ apart. This screened Coulomb potential is scaled in terms of energy unit E_0 defined in Table I. [elaborate for students $F_{Coulomb} == kq_1q_2/r^2$, check scaling/units]. $\kappa = 1/R_0$ is the screening parameter that describes the length scale at which particles interact. We fix the screening length scale R_0 to be a_0 (i.e. unity in simulation units). In experiments charge screening is observed due to ions in the suspending fluid and the charges of surrounding particles which reduces the interaction range of individual particles. Because the particles interact over short ranges, the numerical models can be run efficiency using a neighbor list algorithm determined using a cell method. [explain and reference!]

Newton's second law can be rearranged to the equation of motion a single particle subject to collective effects is

$$\eta\vec{v}_i = \vec{F}_i^l + \sum_{i\neq j}^{N} \vec{F}_{ij} + \vec{F}_D(t). \tag{11}$$

The initial configuration of the system is shown in Fig. 4(a). We annealed the system into a ground-state configuration by raising the system to a high temperature T, and slowly lowering the temperature in steps of $dT = -0.01$ until the particles form a buckled chain in the low region of the channel due to the competition between particle repulsion and channel confinement. The interparticle forces between neighboring particles cause the system to form a buckled chain. The molecular dynamics of simulated annealing is described in Ref. **??**. Once the ground state particle configuration is obtained, no further annealing is necessary, so the our simulations begin with particle configurations that result from the annealing process, as listed in Appendix [ref] and available in supplementary material.

When a single particle is driven, the neighboring particles act similarly to a periodic landscape to impede its motion. A driven particle can exhibit mode locking with a well-chosen ac drive and frequency. In the attached movie, Figure2.mp4, we show the complex dynamics of mode locking, where the driven particle leap-frogs past the other particles.

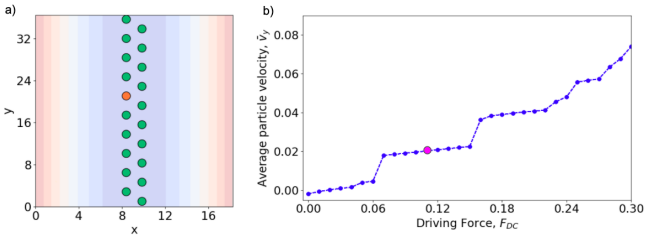

FIG. 4: **(a)** A single particle (colored orange - mark in some manner for non-color views) is driven with a constant amplitude F^{ac} and frequency ω through 19 neighboring particles (colored green - mark differently) confined by a quasi one-dimensional channel. The landscape is colored as in Fig. **??**(a). **(b)** Average $\langle v_y\rangle$ versus F^{dc}, where $\langle v_y\rangle$ is the average particle velocity of the driven particle in the y-direction.

IX. KINKED SYSTEM

We confine N particles to $N-1$ troughs to create a local high density region. $F^{dc}/F^{ac} = 1$ [CHECK!]

Acknowledgments

We acknowledge Harvey Gould and Jan Tobochnik, who invited us to write the article and supported its development. Charles and Cynthia Reichhardt advised the project and provided the original molecular dynamics code written in the C programming language. We acknowledge funding from the M.J. Murdock Charitable Trust and the Pacific Research Institute for Science and Mathematics (PRISM).

[1] A. Pikovsky, M. Rosenblum, and J. Kurths, *Synchronization: A Universal Concept in Nonlinear Sciences* (Cambridge Univ. Press, Cambridge, 2003).

[2] M. Bennett, M.F. Schatz, H. Rockwood, and K. Wiesenfeld, Huygens' clocks, Proc. Roy. Soc. A **458**, 563 (2002).

[3] K. Okamoto, A. Kijima, Y. Umeno, and H. Shima. Synchronization in flickering of three-coupled candle flames. Sci Rep **6**, 36145 (2016)

[4] T. Arane, A. K. R. Musalem and M. Fridman, Coupling between two singing wineglasses, Am. J. Phys. **77**, 1066 (2009).

[5] J. Jia, Z. Song, W. Liu, J. Kurths, and Xiao, J. Experimental study of the triplet synchronization of coupled nonidentical mechanical metronomes. Sci. Rep. **5**, 17008 (2015).

[6] S. Portugal, T. Hubel, J. Fritz, S. Heese, D. Trobe, B. Voelkl, S. Hailes, A. M. Wilson and J. R. Usherwood. Upwash exploitation and downwash avoidance by flap phasing in ibis formation flight. Nature **505**, 399 (2014).

[7] I. Aihara, T. Mizumoto, T. Otsuka, H. Awano, K. Nagira, H. G. Okuno and K. Aihara. Spatio-Temporal Dynamics in Collective Frog Choruses Examined by Mathematical Modeling and Field Observations. Sci Rep **4**, 3891 (2014).

[8] P. Tranchant, D. T. Vuvan, and I. Peretz, Keeping the Beat: A Large Sample Study of Bouncing and Clapping to Music. PLoS ONE 11(7): e0160178. (2016).

[9] G. Martin Hall, Sonya Bahar, and Daniel J. Gauthier, Prevalence of Rate-Dependent Behaviors in Cardiac Muscle. Phys. Rev. Lett. **82**, 2995 (1999).

[10] W. Singer. Striving for coherence. Nature, **397** 391, 1999.

[11] Dutta, S., Parihar, A., Khanna, A. et al. Programmable coupled oscillators for synchronized locomotion. Nat Commun **10**, 3299 (2019).

[12] P. Bak. The Devil's Staircase. Physics Today **39**, 12, 38 (1986).

[13] J. A. Lissajous. "Mmoire sur l'Etude optique des mouvements vibratoires," Annales de chimie et de physique, 3rd series, 51 (1857) 147-232

[14] E. Y. C. Tong, Lissajous figures, The Physics Teacher **35**, 491 (1997).

[15] E. M. Purcell, Life at low Reynolds numbers, Am. J. Phys. **45**, 311 (1977).

[16] B. D. Josephson, Phys. Letters **16**, 25 (1962).

[17] B. D. Josephson, Advan. Phys. **14**, 419 (1965).

[18] W. C. Stewart CURRENTVOLTAGE CHARACTERISTICS OF JOSEPHSON JUNCTIONS Appl. Phys. Lett. 12, 277 (1968).

[19] S. Shapiro, Josephson currents in superconducting tunneling: the effect of microwaves and other observations, Phys. Rev. Lett. 11, 80 (1963).

[20] S. P. Benz, M. S. Rzchowski, M. Tinkham, and C. J. Lobb, Fractional giant Shapiro steps and spatially correlated phase motion in 2D Josephson arrays, Phys. Rev. Lett. 64, 693 (1990); D. Domnguez and J. V. Jose, Giant Shapiro steps with screening currents, Phys. Rev. Lett. 69, 514 (1992).

[21] A. A. Golubov, M. Yu. Kupriyanov, and E. Ilichev. The current-phase relation in Josephson junctions, Rev. Mod. Phys. **76**, 411 (2004).
quote: Phase engineering techniques are used to control the dynamics of long-bosonic Josephson-junction arrays built by linearly coupling Bose-Einstein condensates.

[22] Dengling Zhang, Haibo Qiu, and Antonio Muoz Mateo, Unlocked-relative-phase states in arrays of Bose-Einstein condensates, Phys. Rev. A **101**, 063623 (2020).

[23] C. Reichhardt and C. J. Olson Reichhardt, Depinning and nonequilibrium dynamic phases of particle assemblies driven over random and ordered substrates: a review, Rep. Prog. Phys. 80, 026501 (2017).

[24] C. Reichhardt, and C. J. O. Reichhardt, Shapiro steps for skyrmion motion on a washboard potential with longitudinal and transverse ac drives. Phys. Rev. B **92**, (22). (2015).

[25] M. P. N. Juniper, A. V. Straube, R. Besseling, D. G. A. L. Aarts, and R. P. A. Dullens, Microscopic dynamics of synchronization in driven colloids. Nat. Commun. 6, 7187 (2015).

[26] Juniper, M. P. N., Zimmermann, U., Straube, A. V., Besseling, R., Aarts, D. G. A. L., Lwen, H., and Dullens, R. P. A. Dynamic mode locking in a driven colloidal system: Experiments and theory. New Journal of Physics, 19(1). (2017).

[27] S. Herrera-Velarde and R. Castaeda-Priego, Superparamagnetic colloids confined in narrow corrugated substrates, Phys. Rev. E **77**, 041407 (2008).

[28] S. Herrera-Velarde and R. Castaeda-Priego, J. Phys.: Condens. Matter 19, 226215 (2007).

[29] D. G. Grier, A revolution in optical manipulation. Nature **424**, 810 (2003).

[30] Arthur Ashkin, Optical trapping and manipulation of neutral particles using lasers, Proc. Natl. Acad. Sci. U.S.A. 94, 48534860 (1997).

[31] G. Volpe and G. Volpe, Simulation of a Brownian particle in an optical trap, Am. J. Phys. 81 (3), March 2013

[32] C. Lutz, M. Kollmann, and C. Bechinger, Phys. Rev. Lett. **93**, 026001 (2004); C. Lutz, M. Kollmann, C. Bechinger, and P. Leiderer, J. Phys.: Condens. Matter **16**, S4075 (2004).

[33] S. Tarucha, T. Honda, T. Saku, Solid State Commun. 1995, 94, 413.

[34] A. Gholami, O. Steinbock, V. Zykov, and E. Bodenschatz, Flow-Driven Waves and Phase-Locked Self-Organization in Quasi-One-Dimensional Colonies of Dictyostelium discoideum, Phys. Rev. Lett. **114**, 018103 (2015).

[35] D. Frenkel and B. Smit, Understanding Molecular Simulation: From Algorithms to Applications (Academic Press, London, 2001).

[36] M. P. Allen and D. J. Tildesley, Computer Simulation of Liquids. Second Edition. Oxford University Press (2017).

[37] J. Taylor, Classical mechanics. University Science Books (2005).

[38] See Figure1.mp4 in appropriate